PHYSICAL REVIEW A **76**, 040701(R) (2007)

Classical calculation of ionization and electron-capture total cross sections in $H^+ + H_2O$ collisions

L. F. Errea,[1] Clara Illescas,[1] L. Méndez,[1] B. Pons,[2] I. Rabadán,[1] and A. Riera[1]

[1]*Laboratorio Asociado al CIEMAT de Física Atómica y Molecular en Plasmas de Fusión, Departamento de Química, Universidad Autónoma de Madrid, Madrid-28049, Spain*

[2]*Centre Lasers Intenses et Applications, UMR 5107 du CNRS, Université de Bordeaux-1, 351 Cours de la Libération, 33405 Talence, France*

(Received 31 July 2007; published 10 October 2007)

We report total cross sections for single ionization and electron capture in H^+ collisions with water molecules at impact energies $25\ \text{keV} < E < 5\ \text{MeV}$. Calculations have been carried out by applying the independent-particle model and the eikonal–classical trajectory Monte Carlo (CTMC) method. We have also estimated fragmentation cross sections by multiplying the partial cross sections by the branching ratios measured in the photoionization experiments of Tan *et al.* [Chem. Phys. Lett. **29**, 299 (1978)].

DOI: 10.1103/PhysRevA.76.040701 PACS number(s): 34.70.+e, 34.50.Fa, 52.20.Hv

Ion collisions with water molecules have been studied in several works because their relevance in the cellular damage by ionizing radiations and their potential importance in radiotherapy with protons. In this respect, it has been found [1] that low-energy electrons produced in the ionization of water molecules by ion impact can lead to DNA strand breaking through the formation of autoionizing states. These collisions are also relevant in the modeling of x-ray emission from cometary atmospheres (see [2]). Previous experimental works have reported total ionization and capture cross sections [3–6] as well as the branching ratios for formation of several dissociation products [7–9] in ionization and capture reactions. Calculations of single ionization cross sections have been carried out by applying the continuum distorted wave–eikonal initial state (CDW-EIS) method [10,11] and Born approximation [12]. Electron capture at low energies ($E < 10$ keV) has been studied in [13] by applying a molecular close-coupling expansion. However, no calculations have been carried out at intermediate energies $25 < E < 200$ keV, where ionization and electron capture are significant, and perturbative methods are not applicable.

In this work we have applied the eikonal–classical trajectory Monte Carlo (CTMC) method (see [14]) together with the independent particle model (IPM) to evaluate single electron capture (SEC) and single ionization (SI) cross sections. In our treatment the projectile follows rectilinear trajectories with impact parameter $\mathbf{b}$ and constant relative velocity $\mathbf{v}$. In the CTMC calculation (see [15]), the motion of the active electron is described by means of a classical distribution function, $\rho(\mathbf{r},\mathbf{p},t;v,b)$, which is discretized by using a set of N independent trajectories where the electron moves in the field created by the projectile and a screened Coulomb potential with effective charge Z_k that approximates the interaction with the molecular core; this yields the Hamiltonian (in atomic units)

$$h_k = \frac{\mathbf{p}^2}{2} - \frac{Z_k}{r_t} - \frac{1}{r_p}, \tag{1}$$

where $\mathbf{p}$ is the electronic momentum and $\mathbf{r}_p$, $\mathbf{r}_t$ are the electronic position vectors with respect to the projectile and the target, respectively.

The ionization and capture reactions take place by removing an electron from the valence shell of the water molecule, therefore we have employed four effective charges Z_k, obtained by fitting the ionization energies, I_k, of the four molecular orbitals of this shell ($2a_1$, $1b_2$, $3a_1$, and $1b_1$),

$$Z_k = \sqrt{2n^2 I_k}, \tag{2}$$

with $n=2$. The energies I_k are those employed in the calculation of ionization cross sections by electron impact of Ref. [16]. For each value of Z_k, a CTMC calculation is carried out yielding the capture and ionization one-electron probabilities p_k^{cap}, p_k^{ion} for removing the electron from the corresponding molecular orbital, and $p_k^{\text{el}} = 1 - p_k^{\text{cap}} - p_k^{\text{ion}}$ is the probability that the electron remains attached to the target. In our treatment the initial electron distribution $\rho_k(\mathbf{r},\mathbf{p},t\to-\infty)$ is a hydrogenic one [17]; in the present calculation it is a linear combination of seven microcanonical distributions, ρ_k^j, with different energies E_j,

$$\rho_k(\mathbf{r},\mathbf{p},t\to-\infty) = \sum_{j=1}^{7} a_k^j \rho_k^j(\mathbf{r},\mathbf{p};E_j), \tag{3}$$

where the coefficients a_k^j have been chosen by fitting the quantal position and momentum distributions, and checked that $\Sigma_j a_k^j E_j \simeq E_k$. When using the hydrogenic distribution, the total ionization cross section is compatible with the Bethe limit [14], although this cross section is in general underestimated [18]. In the present case, we have calculated the one-electron ionization cross sections,

$$\sigma_k^{\text{ion}}(E) = 2\pi \int_0^\infty b p_k^{\text{ion}}(b,E) db, \tag{4}$$

and checked that

$$\sigma_k^{\text{ion}}(E) \sim \frac{K}{I_k} \frac{\ln[E\ (\text{keV})]}{[E\ (\text{keV})]}, \tag{5}$$

with $K \simeq 9.0 \times 10^{-15}$ cm^2/hartree. As an additional check, we have evaluated the one-electron cross sections using the impact parameter first Born approximation, in a basis of Slater-type orbitals (see [18]), with angular momentum quantum numbers $0 \leqslant l \leqslant 5$. We have found differences between

CTMC and Born results smaller than 3% for $1<E<5$ MeV.

To evaluate the multielectronic probabilities, we have applied the independent particle model (IPM), also called independent electron model, with an equivalent electron interpretation [19–21]. Assuming that the two electrons occupying the valence orbital k are equivalent, the probabilities for SEC from the orbital k (P_k^{SEC}), and SI from this orbital (P_k^{SI}), are given by

$$P_k^{\mathrm{SEC}} = 2p_k^{\mathrm{cap}}p_k^{\mathrm{el}}\prod_{j\neq k}(p_j^{\mathrm{el}})^2,$$

$$P_k^{\mathrm{SI}} = 2p_k^{\mathrm{ion}}p_k^{\mathrm{el}}\prod_{j\neq k}(p_j^{\mathrm{el}})^2, \tag{6}$$

and the probabilities for total SEC and SI are

$$P^{\mathrm{SEC}} = \sum_{k=1}^{4} P_k^{\mathrm{SEC}} = 2\sum_{k=1}^{4} p_k^{\mathrm{cap}}p_k^{\mathrm{el}}\prod_{j\neq k}(p_j^{\mathrm{el}})^2,$$

$$P^{\mathrm{SI}} = \sum_{k=1}^{4} P_k^{\mathrm{SI}} = 2\sum_{k=1}^{4} p_k^{\mathrm{ion}}p_k^{\mathrm{el}}\prod_{j\neq k}(p_j^{\mathrm{el}})^2. \tag{7}$$

It can be noted that the simulation of x-ray line emission in [22] employs an effective potential description of the target molecule similar to ours [Eq. (1)], but they approximate the capture probability by the average of the one-electron probabilities p_k^{cap} from the two highest valence orbitals ($1b_1$ and $3a_1$).

Using similar arguments, the transfer ionization (TI) probability is

$$P^{\mathrm{TI}} = 4\sum_{k\neq l} p_k^{\mathrm{cap}}p_l^{\mathrm{ion}}p_k^{\mathrm{el}}p_l^{\mathrm{el}}\prod_{j\neq k,l}(p_j^{\mathrm{el}})^2 + 2\sum_{k} p_k^{\mathrm{cap}}p_k^{\mathrm{ion}}\prod_{j\neq k}(p_j^{\mathrm{el}})^2. \tag{8}$$

However, it is well known (see [23] and references therein) that two-electron processes, such as TI, are not accurately described by the IPM, and we have only used this expression as an indication of the importance of this process.

Since our treatment employs a central effective potential to describe the interaction between the electron and the molecular core, it does not take into account the anisotropy of this interaction. To incorporate this effect in the total cross sections we have extended to the present case the method proposed in Ref. [14]. In this model, we assume that the minimum value of the impact parameter is equal to the dimension of the target nuclear skeleton, d, in the direction of $\hat{\mathbf{b}}$. We place the O nucleus on the origin, where it is also centered the effective potential; the H nuclei lie on the YZ half plane with $Z<0$ and the molecular symmetry axis on the Z axis. To average the cross sections over the orientation of the vector $\mathbf{v}$, which is equivalent to average over the molecular orientations with a fixed $\hat{\mathbf{v}}$, we consider a set of 12 trajectory orientations, which correspond to the six-point Cotes formula for the integration over the solid angle that defines the orientation of $\hat{\mathbf{v}}$ with respect to the C_2 molecular axis; this set includes two trajectories with $\hat{\mathbf{v}}$ parallel to the symmetry axis and $\hat{b}=\hat{Y}$, where we have taken $d=2.873/2a_0$ (the equilibrium H-H distance in the ground state of the water molecule is $2.873a_0$). The other two trajectories have $\hat{b}=-\hat{Z}$, where we have taken for d the distance from the O nucleus to the H-H line ($1.102a_0$). Assuming, as in [14], that the transition probabilities are independent on the trajectory orientation, we obtain the simple expression

$$\sigma^X(E) = 2\pi\int_0^\infty \left[b + \frac{1}{6}(1.436+1.102)\right]P^X(b,E)db, \tag{9}$$

where σ^X is the total cross section for a given process (X=SI, SEC, or TI).

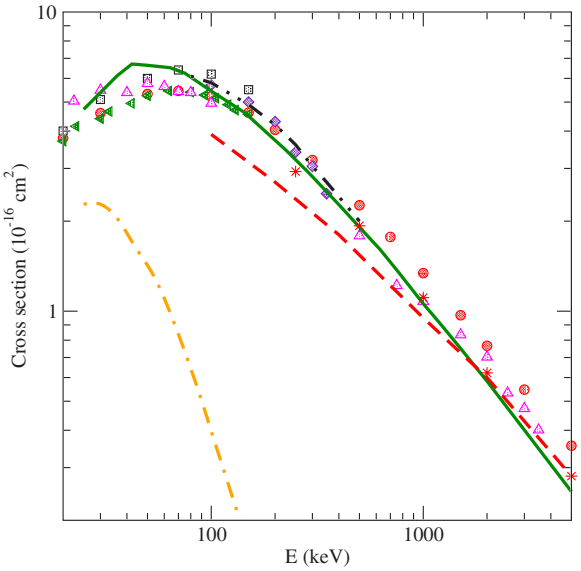

FIG. 1. (Color online) Total cross section for single ionization in proton collisions with H_2O as functions of the impact energy: Full line, present results for SI. Dash-dotted line, present results for TI. Previous calculations: dashed line, [12]; dashed–double-dotted line, [24]; asterisk (∗), [11]. Experimental data for SI: ●, [4]; ■, [5]; ◆, [9]; □ [7]; △ [8]. (The data of Ref. [8] correspond to SI+TI for $15<E<100$ keV and to SI for $E>500$ keV.)

We present in Fig. 1 the total cross section for SI calculated from Eq. (7). As in previous calculations (see [14,25]), the use of the hydrogenic initial distribution is required to accurately describe the ionization threshold; however, in the energy range of Fig. 1, we have found differences with the calculation using the microcanonical distribution (not shown in this figure) smaller than 10%. Our total cross section agrees with the CDW results of Refs. [11,24] and it shows general good agreement with the experimental results of Refs. [9,8] at $E>100$ keV. At $E<100$ keV our calculation overestimates the experimental results. In order to gauge the accuracy of the calculation at low energies, we have included in this figure our estimate of the TI cross section calculated using Eq. (8). As we have already noted, the use of the IPM for two-electron processes is in general not accurate; however, for this particular collision, our result allows us to check that TI is not significant for $E>100$ keV, while at lower energies, the TI cross section is about twice the differ-

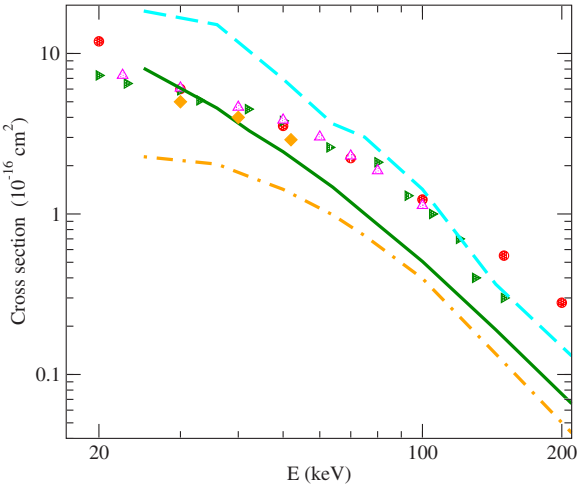

FIG. 2. (Color online) Total cross section for single electron capture in proton collisions with H_2O as functions of the impact energy: Full line, present results for SEC. Dash-dotted line, present results for TI. Dashed line, present results for SEC using the modified IPM treatment of Ref. [28] [see Eq. (10)]. Experimental data for SEC: ●, [4]; ▶, [7]. Experimental data for SEC+TI: ◆, [3]; △, [8].

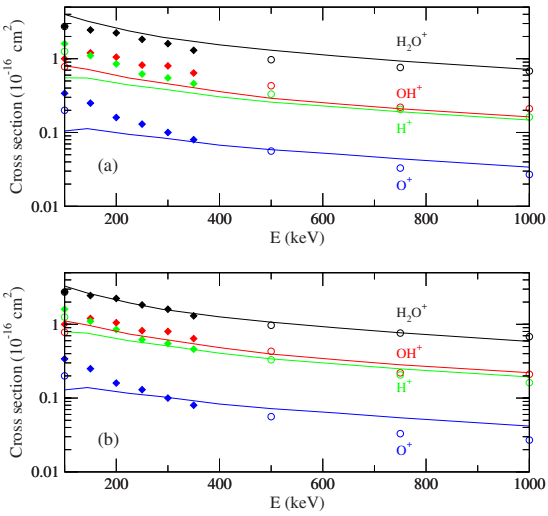

FIG. 3. (Color online) Total cross sections for formation of H_2O^+, OH^+, H^+, and O^+ in the SI reaction, calculated using the branching ratios of Tan *et al.* [29] (a) and Olivera *et al.* [24] (b). Experimental data: ◆, [9], ○, [8].

ence between the experimental values of Refs. [8,7], which can be taken as the experimental estimate of this cross section. The overestimation of the TI cross section by the IPM is similar to that found in ion-atom calculations (see [26]). Since, as we have already mentioned, the influence on the final results of the initial distribution is relatively small, the main limitation of our calculation at low energies is the simple Coulomb potential employed for the electron-H_2O^+ interaction.

With respect to the SEC cross section, we have found differences between microcanonical and hydrogenic calculations that are unnoticeable in Fig. 2; in particular they are smaller than 5% for $25 < E < 100$ keV. The comparison with the experimental cross sections is shown in this figure, where we have restricted the range of impact energies to $E < 200$ keV, where experimental data are available, given the small values of this cross section at higher energies. In order to compare our results with the experimental ones it must be noted that there are significant differences between the available experimental results. In particular, the experiment of Ref. [8] that measured the cross section for SEC+TI reaction yielded almost the same cross sections as those reported in Refs. [4,7] for SEC although, according to the ionization results of Fig. 1, the cross section for TI is not negligible. The comparison between our cross sections and Refs. [4,7] is less satisfactory than for ionization, but the difference between our results and those of Luna *et al.* [8] could be explained as due to the contribution of the TI reaction. In fact the values of SEC and TI cross section in Fig. 2 are similar and the sum of both cross sections roughly reproduces the energy dependence of the experimental results of Ref. [8].

Previous calculations [27,28] for electron capture in collisions of protons with many-electron atoms have suggested that calculated SEC cross section is underestimated because of the unphysical large values of two-electron transitions, and we have considered this possibility for the present case. In particular, the formalism of Kirchner *et al.* [28] yields the following for electron capture in $H^+ + H_2O$:

$$P^{\mathrm{SEC}} = 2\sum_{k=1}^{4} P_k^{\mathrm{cap}}. \tag{10}$$

The use of expression (10) leads to the total SEC cross section plotted in Fig. 2 and we practically obtain the same cross section (not shown in Fig. 2) by employing the modified IPM of [27]. One can note that the cross section calculated using Eq. (10) is very similar to the sum of SEC and TI cross sections from Eqs. (7) and (8) for $E \gtrsim 60$ keV; this can be easily understood since Eq. (10) is obtained by adding the transfer ionization ($p_k^{\mathrm{cap}} p_k^{\mathrm{el}} p_j^{\mathrm{ion}}$) and double capture ($p_k^{\mathrm{cap}} p_k^{\mathrm{el}} p_k^{\mathrm{cap}}$) probabilities to the SEC probability (7) and assuming $p_k^{\mathrm{el}} = 1$, but the TI cross section calculated using this formalism is even larger than that from the usual IPM.

To evaluate the fragmentation cross sections (Fig. 3), we have assumed, as in previous works (see [24]), that the fragmentation takes place as a secondary process after the electron removal from H_2O; this allows us to evaluate the corresponding cross sections by multiplying the ionization probabilities P_k^{SI} from Eq. (6) by the branching ratios obtained in the photoionization experiment of Tan *et al.* [29] and the alternative set of probabilities deduced in [24] in order to obtain good agreement between the experimental cross sections and those obtained from the CDW-EIS total cross sections. We have restricted the energy range to $E > 100$ keV/amu, where TI is not relevant, since, as mentioned in Ref. [8], a different fragmentation pattern is expected when the H_2O^{2+} ion is formed. Besides, the neglect of postcollisional effects becomes less accurate as E decreases. In general we obtain qualitative agreement with the available experiments, and the agreement improves when using the

ad hoc fragmentation probabilities of [24]. In this respect one can notice that the comparison of this partial cross section with the experimental data is a stringent test of our model. Explicitly, the experimental branching ratios were explained in Ref. [30] by taking into account that the Bethe limit of the cross section for ionization from each molecular orbital (5) is proportional to I_k^{-1}. The present calculation incorporates the many-electron structure of the target through the IPM [Eq. (6)], where the ionization probability depends not only on the ionization potential of this orbital, and the modeling of the nonspherical target in Eq. (9). On the other hand, our model cannot provide reliable fragment branching ratios after SEC, given that this process takes place at low energies where TI is significant and since the probabilities deduced from photoionization experiments are probably not appropriate for SEC.

As a conclusion, our calculation shows general good agreement with available experiments, which points to the possibility of applying the CTMC+IPM method to other ion-molecule systems; in particular to collisions with large biomolecules, in the energy range that is relevant in ion-beam cancer therapy, by using effective potentials optimized for these systems, although, as found in collisions with atomic targets, two-electron transitions are not in general well described with the IPM. Our calculation shows that an improved hydrogenic initial distribution, similar to that employed for calculations for collisions with H and H_2, can be constructed for calculations with complex targets.

This work has been partially supported by DGICYT Projects No. ENE2004-06266 and No. FIS2004-04145.

[1] B. Boudaïffa, P. Cloutier, D. Hunting, M. A. Huels, and L. Sanche, Science **287**, 164 (2000).
[2] C. M. Lisse, D. J. Christian, K. Dennerl, K. J. Meech, R. Petre, H. A. Weaver, and S. J. Wolk, Science **292**, 1343 (2001).
[3] R. Dagnac, D. Blanc, and D. Molina, J. Phys. B **3**, 1239 (1970).
[4] M. E. Rudd, T. V. Goffe, R. D. DuBois, and L. H. Toburen, Phys. Rev. A **31**, 492 (1985).
[5] M. A. Bolorizadeh and M. E. Rudd, Phys. Rev. A **33**, 888 (1986).
[6] J. B. Greenwood, A. Chutjian, and S. J. Smith, Astrophys. J. **529**, 605 (2000).
[7] F. Gobet *et al.*, Phys. Rev. A **70**, 062716 (2004).
[8] H. Luna *et al.*, Phys. Rev. A **75**, 042711 (2007).
[9] U. Werner, K. Beckord, J. Becker, and H. O. Lutz, Phys. Rev. Lett. **74**, 1962 (1995).
[10] G. H. Olivera, P. D. Fainstein, and R. D. Rivarola, Phys. Med. Biol. **41**, 1633 (1996).
[11] B. Gervais, M. Beuve, G. H. Olivera, and M. E. Galassi, Radiat. Phys. Chem. **75**, 493 (2006).
[12] O. Boudrioua, C. Champion, C. DalCappello, and Y. V. Popov, Phys. Rev. A **75**, 022720 (2007).
[13] S. Mada, K. N. Hida, M. Kimura, L. Pichl, H.-P. Liebermann, Y. Li, and R. J. Buenker, Phys. Rev. A **75**, 022706 (2007).
[14] C. Illescas and A. Riera, Phys. Rev. A **60**, 4546 (1999).
[15] R. Abrines and I. C. Percival, Proc. Phys. Soc. London **88**, 861 (1966).
[16] W. Hwang, Y.-K. Kim, and M. E. Rudd, J. Chem. Phys. **104**, 2956 (1996).
[17] D. J. W. Hardie and R. E. Olson, J. Phys. B **16**, 1983 (1983).
[18] L. F. Errea, L. Méndez, B. Pons, A. Riera, I. Sevila, and J. Suárez, Phys. Rev. A **74**, 012722 (2006).
[19] J. H. McGuire and L. Weaver, Phys. Rev. A **16**, 41 (1977).
[20] V. Sidorovich, J. Phys. B **14**, 4805 (1981).
[21] H. J. Lüdde and R. M. Dreizler, J. Phys. B **18**, 107 (1985).
[22] S. Otranto, R. E. Olson, and P. Beiersdorfer, J. Phys. B **40**, 1755 (2007).
[23] B. H. Bransden and M. H. C. McDowell, *Charge Exchange and the Theory of Ion-Atom Collisions* (Clarendon, Oxford, 1992).
[24] G. H. Olivera, C. Caraby, P. Jardin, A. Cassimi, L. Adoui, and B. Gervais, Phys. Med. Biol. **43**, 2347 (1998).
[25] L. F. Errea, C. Illescas, L. Méndez, B. Pons, A. Riera, and J. Suárez, J. Phys. B **37**, 4323 (2004).
[26] R. Shingal and C. D. Lin, J. Phys. B **24**, 251 (1991).
[27] B. Hamre, J. P. Hansen, and L. Kocbach, J. Phys. B **32**, L127 (1999).
[28] T. Kirchner, H. J. Lüdde, M. Horbatsch, and R. M. Dreizler, Phys. Rev. A **61**, 052710 (2000).
[29] K. H. Tan, C. E. Brion, P. E. Van der Leeuw, and M. J. Van der Wiel, Chem. Phys. Lett. **29**, 299 (1978).
[30] E. C. Montenegro, S. W. J. Scully, J. A. Wyer, V. Senthil, and M. B. Shah, J. Electron Spectrosc. Relat. Phenom. **155**, 81 (2007).